Synthesis of CoFe/Al2O3 composite nanoparticles as the impedance matching layer of wideband multilayer absorber

L. Zhen, Y. X. Gong, J. T. Jiang, C. Y. Xu, W. Z. Shao, P. Liu, and J. Tang

Citation: Journal of Applied Physics **109**, 07A332 (2011); doi: 10.1063/1.3564939
View online: http://dx.doi.org/10.1063/1.3564939
View Table of Contents: http://scitation.aip.org/content/aip/journal/jap/109/7?ver=pdfcov
Published by the AIP Publishing

Synthesis of $CoFe/Al_2O_3$ composite nanoparticles as the impedance matching layer of wideband multilayer absorber

L. Zhen,[1,2,a)] Y. X. Gong,[1] J. T. Jiang,[1] C. Y. Xu,[1,2] W. Z. Shao,[1] P. Liu,[3] and J. Tang[3]
[1]*School of Materials Science and Engineering, Harbin Institute of Technology, Harbin 150001, People's Republic of China*
[2]*MOE Key Laboratory of Micro-systems and Micro-structures Manufacturing, Harbin Institute of Technology, Harbin 150001, People's Republic of China*
[3]*Department of Physics and Anstronomy, University of Wyoming, Laramie, Wyoming 82071, USA*

(Presented 17 November 2010; received 21 September 2010; accepted 6 December 2010; published online 13 April 2011)

$CoFe/Al_2O_3$ composite nanoparticles were successfully prepared by hydrogen-thermally reducing cobalt aluminum ferrite. Compared with CoFe alloy nanoparticles, the permeability of $CoFe/Al_2O_3$ composite nanoparticles was remarkably enhanced and an improved impedance characteristic was achieved due to the introduction of insulated Al_2O_3. A multilayer absorber with $CoFe/Al_2O_3$ composite nanoparticles as the impedance matching layer and CoFe nanoflake as the dissipation layer was designed by using genetic algorithm, in which an ultrawide operation frequency bandwidth over 2.5–18 GHz was obtained. The microwave absorption performance in both normal and oblique incident case was evaluated by using electromagnetic simulator. The backward radar cross-section (RCS) was decreased at least 10 dB over a wide frequency range by covering the multilayer absorber on the surface of perfect electrical conductive plate. © *2011 American Institute of Physics*. [doi:10.1063/1.3564939]

I. INTRODUCTION

Microwave absorber with ultrawideband performance is urgently demand in the fields of "Stealth" technology and wireless communication systems,[1,2] in which the absorber is used to reduce the radar cross section (RCS) of aircrafts and resolve electromagnetic interference problems. It is well known that the electromagnetic absorption (EMA) performance of the absorber is determined by the impedance characteristics and intrinsic EM dissipation efficient, which determines how much energy can be penetrated into the absorber and dissipated inside the absorber, respectively. Although plenty of effort has been paid on the development of novel filler materials to tailor the electromagnetic properties, both of high dissipation efficient and good impedance matching is difficult to be achieved simultaneously for the monolayer absorbers with sole filler materials in a wide frequency band. And thus, few of monolayer absorbers have achieved a sufficiently wide bandwidth that satisfies the requirements set forth in a wide variety of applications.[3]

The multilayer absorbers composed of dissipation part and impedance matching part, which is realized by adopting different materials with distinct electromagnetic characteristic as fillers of each unit layer, is believe to be more promising for wideband applications than it does as the monolayer absorber.[4,5] Generally, the filler materials for dissipation part is required to possess high dielectric or magnetic dissipation factor, which is relatively easy to be achieved in some commercial materials with high dielectric loss tangent, such as carbon nanotubes (CNTs), SiC whisker, and so on.[6,7] As another important component, the permittivity and permeability of impedance matching part should be close to each other to ensure the characteristic impedance is well matched with that of free space. Since the microwave permeability of natural materials is usually lower than permittivity, the magnetic materials such as ferromagnetic alloy/oxidation composite nanoparticles with high microwave permeability and suitable permittivity are promising candidates for impedance matching materials. It is well known that the Snoek's limitation and eddy current effect are two key factors which results in the deterioration of permeability in microwave region. The high saturation magnetization of ferromagnetic alloy is beneficial to increase the Snoek's cut-off frequency. Meanwhile, the introduction of insulated oxidation would decrease the conductivity and thus suppress the eddy current effect. Therefore, higher microwave permeability is achieved much more easily in the ferromagnetic alloy/oxidation composite nanoparticles rather than the traditional ferrite and ferromagnetic alloy powders.

In this paper, $CoFe_x/Al_2O_3$ composite nanoparticles with different Co:Fe relative content were synthesized by hydrogen-thermally reducing cobalt aluminum ferrite. The effect of ferromagnetic component ratio on the electromagnetic properties was studied. An ultrawideband multilayer absorber with $CoFe_3/Al_2O_3$ as impedance matching layer is designed by genetic algorithm (GA) optimization. Moreover, the RCS reduction efficient and performance in oblique incident case is studied by using electromagnetic simulator.

II. EXPERIMENTAL

First, the precursor $CoFe_xAl_{2-x}O_4$ particles were prepared with a facile hydrothermal process as described in our previous work.[8] Herein, the ratio of Co:Fe (1:x) and content of insulated Al_2O_3 was controlled by varying the relative concentration of reactants. And then, $CoFe_x/Al_2O_3$ composite nanoparticles were synthesized by reducing the precursor

a)Electronic mail: lzhen@hit.edu.cn.

$CoFe_xAl_{2-x}O_4$ particles in hydrogen atmosphere at 500 °C for 120 min. The reduced products were cooled in N_2 atmosphere to room temperature naturally in furnace.

A multilayer absorber with the prepared $CoFe_x/Al_2O_3$ composite nanoparticles as filler materials of impedance matching layer and CoFe nanoflakes (CoFe NFs)[9] as filler materials of dissipation layer is designed by using GA method, in which the thickness of each unit layer is optimized to obtain the widest effective absorption frequency bandwidth (BW_{eff}). The BW_{eff} is defined as the operation frequency bandwidth in which the reflection coefficient of absorber backed with perfect electrical conductive (PEC) plate is less than −10 dB.

The EM parameters of the composites containing $CoFe_x/Al_2O_3$ composite nanoparticles (20 vol.%) and paraffin (80 vol.%) were measured on a vector network analyzer (VNA, N5230A) on transmission/reflection mode. The EMA performance in the case of oblique incidence and RCS reduction efficient with PEC background was evaluated by using electromagnetic simulation software GEMS.

III. RESULTS AND DISCUSSION

Figure 1 shows the XRD patterns of the precursor cobalt alumina ferrite and reduced $CoFe_3/Al_2O_3$ composite nanoparticles. The diffraction peaks in the pattern of precursor ferrite can be indexed to $CoFe_2O_4$ phase (JCPDS: 1-1121) with spinel structure. Meanwhile, a slight peak shift compared with the standard diffraction card can be observed which is speculated to be caused by the replacement of Fe^{3+} position in the spinel structure by Al^{3+}. As indicated in the pattern of reduced product, both diffraction peaks corresponding to CoFe alloy (JCPDS: 48-1816) and Al_2O_3 phase (JCPDS: 2-291) are observed, which confirms the formulation of $CoFe_x/Al_2O_3$ composite structure in the hydrogen-thermal reductions.

Figure 2(a) and 2(b) shows the SEM images of the precursor ferrite particles and reduced $CoFe_3/Al_2O_3$ composite nanoparticles. The precursor ferrite particles are spherelike and about 100 nm in diameter. The diameter of reduced $CoFe_3/Al_2O_3$ composite nanoparticles is similar to the precursor ferrite particles and no serious agglomeration is found, which is different from the CoFe alloy particles without Al_2O_3 phase prepared in our previous work.[8] As shown in Fig. 2(c), although the reduction duration is shorter,

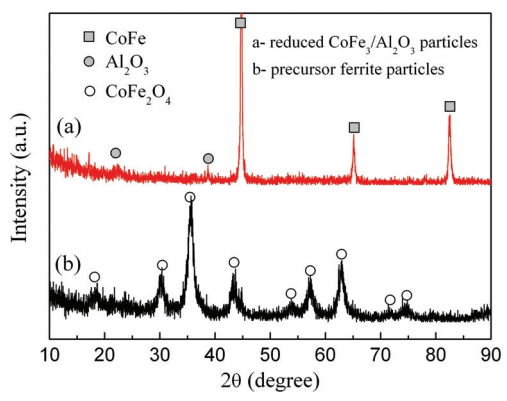

FIG. 1. (Color online) XRD patterns of precursor ferrite and reduced $CoFe_3/Al_2O_3$ composite nanoparticles.

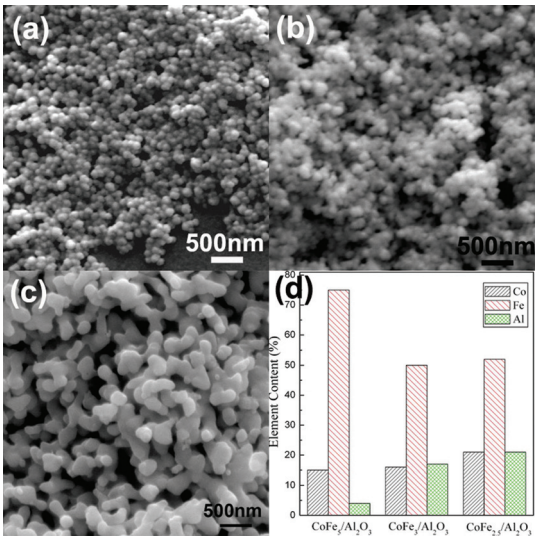

FIG. 2. (Color online) SEM images of (a) precursor ferrite particles; (b) reduced $CoFe_3/Al_2O_3$ composite particles; (c) CoFe alloy nanoparticles; (d) EDS analysis of reduced $CoFe_x/Al_2O_3$ composite particles with different x values.

a serious agglomeration among the reduced CoFe alloy particles can be clearly observed and the particle size is remarkably enlarged. For the $CoFe_3/Al_2O_3$ composite nanoparticles, the existence of Al_2O_3 phase plays an important role as a "frame" to prevent the agglomeration phenomenon during the hydrogen-thermal reduction, which ensures the morphology of reduced particle controllable at high temperature. As indicated in Fig. 2(d), the energy dispersive spectrometer (EDS) analysis demonstrates that the relative content of ferromagnetic component (Co:Fe) increases with x value varied from 1:2.5 to 1:5, and accordingly the content of Al_2O_3 decrease with the increase of x value.

The saturation magnetization (M_s) and coercivity (H_c) of $CoFe_x/Al_2O_3$ composite nanoparticles with different x values were measured. Due to the increase of relative content of Fe with higher saturation magnetization and decrease of nonmagnetic component Al_2O_3, the saturation magnetization and coercivity of $CoFe_x/Al_2O_3$ composite nanoparticles is found to increase from 121.38 emu/g and 352.06 Oe of $CoFe_{2.5}/Al_2O_3$ to 150.21 emu/g and 553.47 Oe of $CoFe_5/Al_2O_3$.

The complex permittivity and permeability spectrums of specimen containing $CoFe_x/Al_2O_3$ composite nanoparticles with different x values as fillers are plotted versus frequency and shown in Fig. 3. As indicated in the permittivity spectrums, the real part of permittivity (ε') of $CoFe_{2.5}/Al_2O_3$ and $CoFe_5/Al_2O_3$ remains around 6 and 7.5 in the frequency band of 2–18 GHz. In contrast, the ε' of $CoFe_3/Al_2O_3$ decreases from 7.5 to 6 with the increase of frequency, which is lower than that of $CoFe_5/Al_2O_3$ and higher than that of $CoFe_{2.5}/Al_2O_3$ all through the frequency band of 2–18 GHz, respectively. Herein, the decrease of ε' is speculated to be resulted from the increase of insulated component Al_2O_3 and consequently decrease of conductive component CoFe alloy with the decrease of x values. Since the dielectric properties are usually determined by the interfacial polarization of free charge on the conductor/insulator interface for the composites with conductive particles dispersed in an insulated matrix, the decrease of conductive CoFe alloy particles would

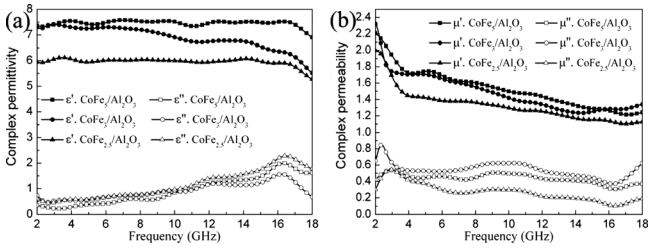

FIG. 3. Complex permittivity and permeability of specimen containing $CoFe_x/Al_2O_3$ composite nanoparticles with different x values as fillers, respectively, (a) the complex permittivity spectrum; (b) complex permeability spectrum.

lead to the decrease of such conductor/insulator interfacial polarization, and thus the ε' of $CoFe_{2.5}/Al_2O_3$ is lower than that of $CoFe_3/Al_2O_3$ and $CoFe_5/Al_2O_3$.

As indicated in Fig. 3(b), the real part of permeability (μ') of $CoFe_3/Al_2O_3$ decreases gently from 2.32 to 1.33 in the frequency band of 2–18 GHz, which is remarkably higher than that of CoFe alloy nanoparticles with a similar particle size and higher M_s value as reported in our previous work.[9] The improvement of permeability of $CoFe_3/Al_2O_3$ composite nanoparticles should be ascribed to the introduction of insulated Al_2O_3, which is beneficial to decrease the conductivity and thus suppress the eddy current effect. Actually, the conductivity is in fact confirmed to decrease from 7.8×10^5S/m of CoFe alloy nanoparticles to 0.23×10^{-4} S/m of $CoFe_3/Al_2O_3$ composite nanoparticles, where the conductivity is obtained by using four-probe conductivity measurement method. Moreover, an obvious controlling function of relative content of Al_2O_3 is found on the magnetic properties of $CoFe_x/Al_2O_3$ composite nanoparticles. Since the relative content of Fe: Co increases with the decrease of Al_2O_3, the M_s of $CoFe_x/Al_2O_3$ composite nanoparticles increases with x value. Therefore, the μ' of $CoFe_x/Al_2O_3$ is observed increase with x value due to the increase of M_s.

Subsequently, a multilayer absorber adopting the impedance matching layer with $CoFe_3/Al_2O_3$ as fillers on the top and dissipation layers containing CoFe NFs as fillers on the bottom is designed and the thickness of each unit layer is optimized by using GA method. The EMA performance of multilayer absorber and corresponding monolayer absorbers containing, respectively, $CoFe_3/Al_2O_3$ and CoFe NFs as fillers is shown in Fig. 4. As indicated in Fig. 4(a), due to the good impedance matching characteristic of $CoFe_3/Al_2O_3$ which is originated from the high permeability and suitable permittivity, a BW_{eff} of 10–18 GHz is achieved which is about 2 GHz wider than that of the reported CoFe alloy nanoparticles. However, because of the low intrinsic dissipation efficient, the reflection coefficient of the monolayer $CoFe_3/Al_2O_3$ absorber remains in a high level in the frequency band of 2–10 GHz. Similarly, although the intrinsic dissipation efficient of CoFe NFs is high as reported in reference,[9] the BW_{eff} is narrow and just covers the frequency range of 3–4 GHz because of the poor impedance matching characteristic. Whereas, the good impedance matching characteristic of $CoFe_3/Al_2O_3$ and high dissipation efficient of CoFe NFs is well integrated and an ultrawideband BW_{eff} over the frequency range of around 2.5–18 GHz is obtained in the multilayer absorber, and the reflection coefficient remains less than −15 dB in the frequency band of 5–15 GHz.

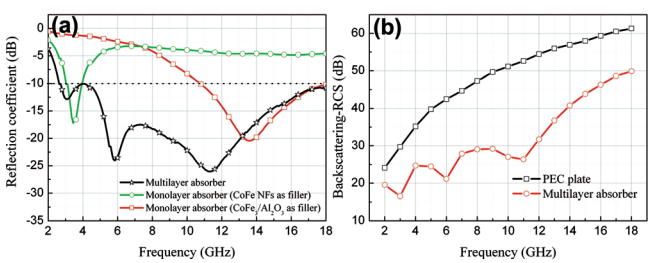

FIG. 4. (Color online) EMA performance of multilayer absorber backed with PEC plate. Reflection coefficient spectrum; (b) backward-scattering RCS result.

Moreover, the backward scattering RCS of the multilayer absorber backed with finite PEC plate of (300×300 mm^2) is evaluated by using electromagnetic simulation software GEMS. The backward scattering RCS is decreased at least 10 dB over an ultrawide bandwidth of 3–18 GHz by coating the multilayer absorber on the surface of PEC plate. And a decrease of RCS exceeding 20 dB around 6 and 11 GHz is achieved, which is well in accordance with the absorption peaks indicated in the reflection coefficient spectrum.

IV. CONCLUSIONS

In the present work, $CoFe/Al_2O_3$ composite nanoparticles with different relative content of ferromagnetic component are synthesized by a hydrogen-thermally reducing cobalt aluminum ferrite. Compared with the CoFe alloy nanoparticles, the introduction of simulated Al_2O_3 effectively prevents the agglomeration during the reduction process. Additionally, a remarkably microwave permeability and improved impedance matching characteristic is achieved in $CoFe/Al_2O_3$ composite nanoparticles. An ultrawideband absorption performance covering the frequency band of 2.5–18 GHz is obtained in a GA optimized multilayer absorber with $CoFe/Al_2O_3$ composite nanoparticles as fillers of impedance matching layer. The backward scattering RCS is revealed to decrease at least 10 dB over the frequency band of 3–18 GHz after covering the multilayer absorber on the surface of 300×300 mm^2 PEC plate.

ACKNOWLEDGMENTS

This work was financially supported by Program of Excellent Team at HIT.

[1]J. L. Wallce, IEEE Trans. Magn. **29**, 4209 (1993).
[2]J. T. Jiang, L. Zhen, B. Y. Zhang, W. Z. Shao, and C. Y. Xu, Scripta. Mater. **59**, 967 (2008).
[3]S. S. Kim, S. T. Kim, Y. C. Yoon, and K. S. Lee, J. Appl. Phys. **97**, 10F905 (2005).
[4]H. Cui, H. Ling, and C. S. Liang, IEEE Trans. Antennas Propagat. **56**, 2127 (2008).
[5]S. Cui and D. S. Weile, IEEE Trans. Antennas Propagat. **53**, 3616 (2005).
[6]J. T. Jiangi, L. Zhen, C. Y. Xu, and W. Z. Shao, Surf. Coat. Technol. **201**, 6059 (2007).
[7]J. T. Jiangi, L. Zhen, C. Y. Xu, and X. L. Wu, Surf. Coat. Technol. **201**, 3139 (2006).
[8]Y. X. Gong, L. Zhen, J. T. Jiang, C. Y. Xu, and W. Z. Shao, J. Magn. Magn. Mater. **321**, 3702 (2009).
[9]Y. X. Gong, L. Zhen, J. T. Jiang, C. Y. Xu, and W. Z. Shao, J. Appl. Phys. **106**, 064302 (2009).